Iraqi Journal of Physics, 2021 *Vol.19, No.48, PP. 33-43*

DOI: 10.30723/ijp.19.48.33-43

Antibacterial and Morphological Properties of Polypyrrole/Silver Nanocomposites Synthesized by Chemical Oxidation Polymerization

Mohammed Abdilridha Salman, Salma M. Hassan

Department of Physics, College of Science, University of Baghdad, Baghdad, Iraq

E-mail: salma.mhammed@yahoo.com

Corresponding author: mohammed.a.salman@outlook.com

Abstract

Polypyrrole/silver (PPy/Ag) nanocomposites of weight percentages (0.1%, 0.5%, 3%, 5% and 7% wt.) were synthesized via a chemical oxidation method. The AFM analysis is performed to study the surface roughness, morphology and size distribution of PPy particles and PPy-Ag nanocomposites. The results indicated that as the concentration of Ag in the nanocomposite increases, the roughness increases. The size of nanoparticles was also evaluated and found to be in the range of 15 nm to 125 nm. The PPy/Ag nanocomposites exhibited an effectiveness against Gram-negative Escherichia coli showing an inhibition zone of 4mm and displayed poor efficacy against Gram-positive Staphylococcus aureus. Based on given adequate antibacterial characteristics of PPy/Ag nanocomposites, it can be identified as a promising material in biomedical applications.

Key words

Polypyrrole, silver nanoparticles, nanocomposite; morphology, antibacterial mechanism.

Article info.

Received: Sep. 2020
Accepted: Dec. 2020
Published: Mar. 2021

الخصائص المضادة للبكتيريا والمورفولوجية للمركبات النانوية للبوليبايرول / الفضة المصنعة بواسطة البلمرة المؤكسدة الكيميائية

محمد عبد الرضا سلمان، سلمى محمد حسن

قسم الفيزياء، كلية العلوم، جامعة بغداد، بغداد، العراق

الخلاصة

تم تصنيع مركبات النانو بوليبايرول / الفضة عن طريق الاكسدة الكيميائية. تم اجراء تحليل ال AFM لدراسة لخشونة السطح والتشكل وتوزيع حجم الجزيئات للبوليبايرول والمتراكبات النانوية البوليبايرول / الفضة. اشارت النتائج الى انه مع زيادة تركيز الفضة في المركب النانوي الخشونة تزداد. تم أيضًا تقييم حجم الجسيمات النانوية ووجد انها في حدود 15 نانومتر إلى 125 نانومتر. أظهرت المركبات النانوية البوليبايرول / الفضة فعالية ضد الإشريكية القولونية سالبة الجرام والتي اظهرت منطقة تثبيط تبلغ 4 مم. وأظهرت فعالية ضعيفة ضد المكورات العنقودية الذهبية إيجابية الجرام. بناءً على الخصائص المضادة للبكتيريا المناسبة لمركبات البوليبايرول / الفضة النانوية ، يمكن تحديدها على أنها مادة واعدة في التطبيقات الطبية الحيوية.

Introduction

Conducting polymers nanocomposites have attracted considerable attention in various academic and industrial fields. Due to their unique and promising properties especially mechanical, electrical and biological ones, It can be applicable in various disciplines including biomedical devices, energy storage and biosensors [1]. Polypyrrole (PPy) is one of numerous conductive polymers that can be characterized by its simple synthesis, excellent biocompatibility and recognizable conductivity in comparison with other conductive polymers [2, 3]. Considering its special

characteristics, PPy and its composites could be used in diverse applications including anticorrosion coatings [4], supercapacitors [5], sensors [6], biosensors [7] and biomedical uses [8]. Antimicrobial polymers, polymers that have the ability to inhibit the growth of microorganism, have the advantage of being non-volatile, chemically stable, and unable to penetrate the skin of humans or animals easily which may increase the effectiveness of some existing antimicrobial agents and reduce environmental issues associated with the residual toxicity of these agents in addition to extending their lifetime [9]. There are several reasons that make PPy a good choice for an antibacterial action such as the high surface area, small particle size, non-volatility, chemical stability and, the active functional group in the main chain of the polymer [10]. In contrast, PPy possess some qualities that need to be improved such as poor mechanical characteristics and processability. This can be done either by attaching side groups to the backbone of the polymer [11], grafting polymers to a non-conductive polymer, developing pyrrole copolymers [12], forming PPy composites or blends with any appropriate polymer that provides enhanced mechanical and chemical properties [13]. The combination of PPy and other materials for the preparation of composites which share the qualities from both materials is a successful way of obtaining specific characteristics for different types of applications [14]. Silver (Ag) is considered as one of the most significant metals to be studied on nanoscale basis, owing to its remarkably high electrical conductivity, notable optical properties that rely heavily on the size and shape of the nanoparticles [15]. Silver nanoparticles (AgNPs) are widely used in numerous fields, such as medical, food, health care, and industrial disciplines, because of their excellent physical and chemical characteristics. [16, 17]. Interest in synthesis of PPy/Ag nanocomposites is tremendously growing interest due to the favorable optical and electrical properties of Ag and the conductive property of the polymer [18]. Additionally, organic polymers have been indicated to be exceptional candidates for trapping metals nanoparticles, based on its ability to serve as stabilizing or surface capping agents [19]. Many initiatives have been made to investigate the impact of reaction conditions on the characteristics and morphology of PPy/Ag nanocomposites. For an anti-bacterial application, Alireza S. et al. [20] fabricated Ag-polypyrrole core-shell nanosphere was fabricated using microemulsion system at room temperature by Alireza S. et al. [20]. The resulting nanocomposite was fully characterized by FT-IR, XRD, TEM and X-ray photoelectron spectroscopy techniques. Results also showed that the Ag nanoparticles were incorporated into the PPy backbone. Evaluation of the anti-bacterial activity against clinical isolates of Gram-positive (Staphylococcus aureus) and Gram-negative (Escherichia coli) was presented by typical effective zones. The objective of this research is to synthesize PPy/Ag nanocomposites via chemical oxidation method. They were synthesized using the same method for different compositions as advanced antimicrobial agents. The morphology of PPy/Ag nanocomposite was characterized by AFM. The biological activity of PPy/Ag was explored against Gram-negative bacteria; E. coli and Gram-positive bacteria; S. aureus by means of disk diffusion method. The article attempts to analyze the antimicrobial activity of PPy and PPy/Ag in both schematics and explanations.

Experimental work

Reagents

Various materials have been used to synthesis both PPY and PPY/Ag nanocomposites. These materials include: (i) pyrrole as a monomer, supplied by FlukaAG doubly distilled and cooled in icy water before use (ii) Ammonium

peroxydisulfate (APS) as an oxidant, provided by (Central Drug House, India) and used without any modifications (iii) Silver nanoparticles (99.9% 10nm) were obtained from American Elements (iv) Hydraulic acid to be diluted and used as cleaning solution for the sample.

Bacteria

The Gram-negative bacteria; E. coli (PTCC 1398) and Gram-positive bacteria; S. aureus (ATCC 25923), supplied by the Alnokhba Laboratory for Medical Diagnostics, was used to evaluate the antibacterial activity of PPy/Ag nanocomposites. These microorganisms were placed in Muller Hinton Agar Medium. The medium was prepared by dissolving 33.9 g of the commercially available Muller Hinton Agar Medium (HiMedia) in 1000ml of distilled water. The dissolved medium was autoclaved at 15 lbs pressure at 121°C for 15 minutes. The autoclaved medium was mixed well and poured onto 100mm Petri dishes (25-30ml/plate) while still molten.

Synthesis of polypyrrole

1.34 ml of pyrrole was placed in a beaker and diluted with 50 ml of distilled water. By doing so, a one molar concentration was obtained. After that, this mixture was poured in a 3 neck round bottom flask, kept under a constant stirring and remained under ice bath at 3 C for 15 minutes. Meanwhile, another solution of 1 M of ammonium peroxydesulphate (APS) was prepared by adding 50 ml of distilled water to 4.58g of such material. Similarly, this solution was retained under constant stirring and at low temperature. The APS solution was then added dropwise to the pyrrole solution. It was observed that the color of the solution had been changed to dark black after being transparent with the appearance of granules. A digital thermometer was dipped into the solution to monitor the temperature change. Soon, the temperature rose from 3 ^{o}C to 17 ^{o}C in less than 10 seconds and started to drop gradually. The polymerization process took a period of 5 h under constant stirring at 3 ^{o}C. In addition, the solution was left to settle for 20 hours.

In the next day, this mixture was filtered under vacuum. Meanwhile, 0.6 ml of hydrochloric acid was added to 50 ml of water and used to wash the mixture. Later, a volume of 50 ml of distilled water was added to the above filtered compound for washing purposes. The resulting compound from the filtration process was dried in an oven at a temperature under 80 ^{o}C for 4 hours. After making sure that the powder was humidity free, it was crushed with a mortar to obtain fine powder for further diagnostic analyses. Fig. 1 demonstrates the black color of PPy powder.

Fig. 1: The image of PPy and PPy/Ag nanocomposites powder.

Synthesis of PPy/Ag nanocomposites

In a similar manner, the distilled pyrrole was used in the preparation process of PPy/Ag nanocomposites as follows.

Ag nanoparticles of weight percentages (0.1%, 0.5%, 3%, 5% and 7% wt.) were weighed by a 4-digit balance in a glove box filled with nitrogen to ensure oxygen-free environment. 1.34 ml of pyrrole was weighed and kept in a beaker. A 50 ml of distilled water was added to pyrrole to acquire one molar concentration. Thereafter, the solution was poured in a 3 neck round bottom flask that was placed under ice bath at 3C with constant stirring for 15 minutes. Afterwards, silver nanoparticles were added to the diluted pyrrole and kept under stirring for 15 minutes. Next, another solution of 1M of ammonium peroxydesulphate (APS) was prepared by dissolving 4.58g into a 50 ml of water. This solution was kept under low temperature. Soon after, the APS solution was added drop wise to the pyrrole solution. This process in illustrated in Fig. 2.

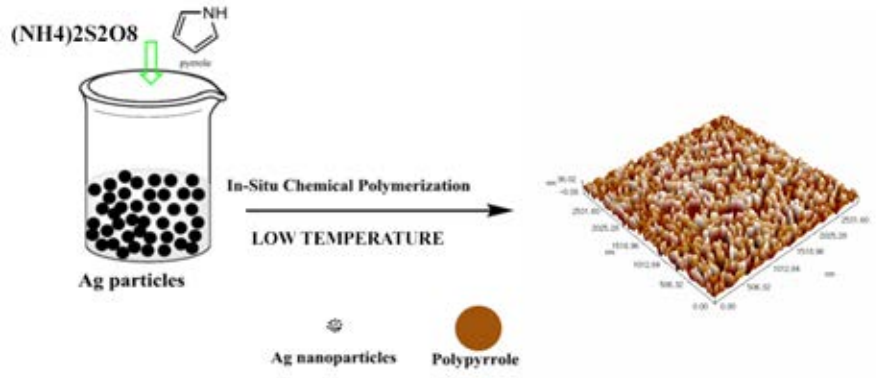

Fig. 2: Schematic representation of formation mechanism of PPy/Ag nanocomposites.

Instrumentation

The morphology, structure and particle size of the PPy/Ag nanocomposites were analyzed with an atomic force microscope (AFM; Zeiss EM10C, Germany, operating at 80 KV). In addition, FTIR spectrophotometer (Shimadzu 8400s series) with (400 cm – 4000 cm), was used to provide the required spectra of pure Polypyrrole and PPy/Ag in powder form.

Results and discussion

Reaction temperature and polymerization time

The PPy and PPy/Ag nanocomposites oxidation reaction temperature varies with polymerization time. This relationship is illustrated in Fig.3 which also indicates the exothermicity of this reaction. As noticed from the figure, there are three distinct stages; the temperature remains virtually constant stage 1 which is called the induction period. It was noticed that the color of the solution has changed, in stage 2, from being transparent to dark black with the appearance of granules which preceded the composition of oligomeric intermediates. Post polymerization stage which is stage 3 begins when the temperature drops and the reaction enters its saturation stage.

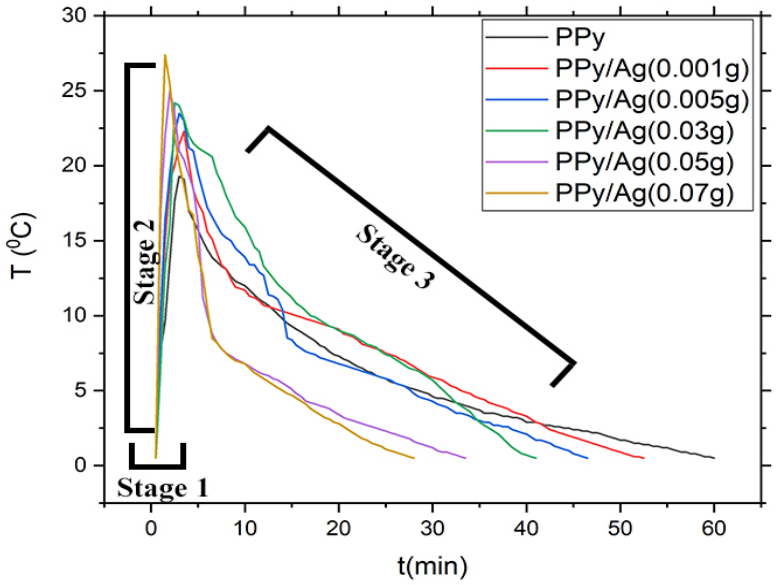

Fig. 3: Polymerization time as a function of reaction temperature for PPy and PPy/Ag nanocomposites.

Conclusions from reaction temperature and polymerization time

It is possible to mention three points concluded from Fig.2:

- The polymerization process for PPy/Ag nanocomposites takes less time than that of pure PPy and this time decreases with the increase in silver nanoparticles concentration.
- As the nanoparticles concentration increase, the maximum temperature of the reaction in increases, and it reaches to a maximum value for PPy/Ag (0.07g).
- Considering the PPy/Ag (0.05g and 0.07g) nanocomposites, the temperature of saturation starts in time earlier than in pure PPy.

These findings can be due to the effect of silver nanoparticles which can raise the temperature of the reaction and accelerate the process of polymerization.

IR spectroscopy

The FTIR spectra of PPy and PPy/Ag (0.1%, 0.5%, 3%, 5% and 7% wt.) nanocomposites are illustrated in Fig.4 (a, b, c, d, e and f). The peaks shown below are believed to validate the chemical composition of PPy [21]. The IR spectra of PPy(Fig.4a) reveals a large band in the range of 3400-3500 cm^{-1} owing to the N-H band of the stacking of monomer ring. [22]. The pyrrole fundamental ring vibration (C = O stretching of the quinone ring) can be allocated to the peak value of 1558 cm^{-1}. The intensity that is observed at 1451 cm^{-1} represents C-C vibration. The peak of 1384 is due to NO_3^- balancing anion [23]. The peaks here around 725-1110 cm^{-1} reflect C-H in the plane and C-H in the plane deformation [24]. Furthermore, it is clear that the amplitude of the N-H stretching vibration between 3400 - 3500 cm^{-1} has reduced which is attributed to the engagement of these groups with the Ag particles, as the NH polymer groups are often located outside the polymer backbone and having to face the electrolyte side [25]. It can be clearly seen that the major PPy peaks haven't shifted, and there is a small or not considerable shift in the minor peaks when adding different concentrations of silver nanoparticles. In addition, the formation of PPy/Ag nanocomposites didn't establish any new peaks to consider.

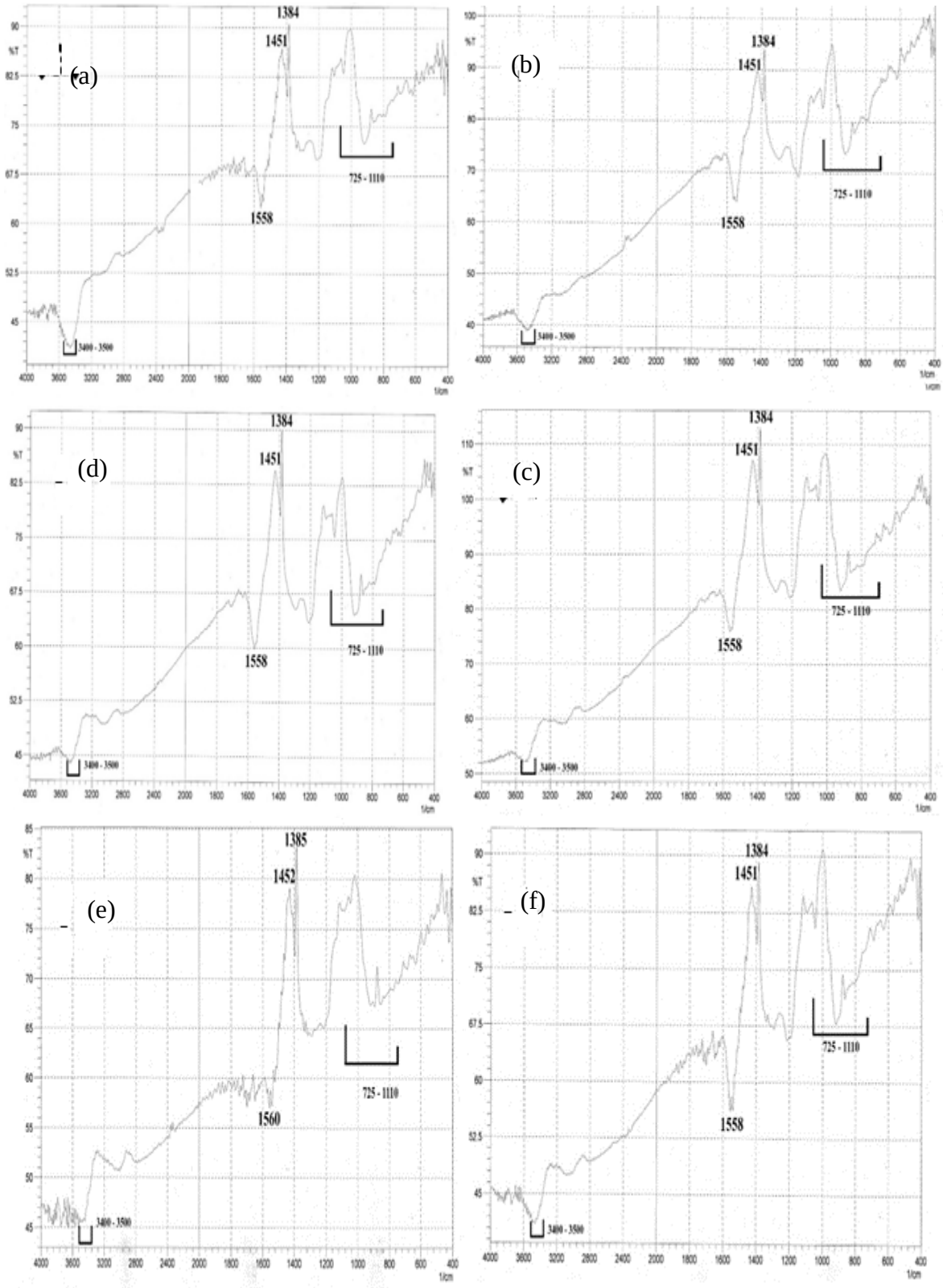

Fig. 4: FTIR analysis of: (a) PPy, (b) PPy/ 0.1% Ag, (c) PPy/ 0.5% Ag, (d) PPy/ 3% Ag, (e) PPy/ 5% Ag, and (f) PPy/ 7%Ag.

Morphology analysis

The AFM analysis was performed in order to study the surface roughness, morphology and size distribution of the PPy particles and PPy-ag nanocomposites. Height - width diagrams were evaluated using Gwydion software. Figs.5 (A1, B1, C1, D1, E1, and F1) shows AFM images of selected areas of pure PPy nanoparticles and PPy/Ag (0.1%, 0.5%, 3%, 5% and 7% wt.) nanocomposites. It can be inferred that a completely amorphous surface is noted which is in agreement with the typical morphology of this material. It can also be noted that the formation of nodules that continue to grow to form tube lines as the weight percentage of the silver nanoparticles increases. Figs.5 (A2, B2, C2, D2, E2, and F2) represent height-width profiles which describe the number of peaks and valleys in the image that significantly affect the average roughness. The results indicated that as the concentration of Ag in the nanocomposite increases, the roughness also increases. The size of nanoparticles was also evaluated and found to be in the range of 15 nm to 125 nm. Figs.5 (A3, B3, C3, D3, E3, and F3) represent the granularity cumulation distribution charts which illustrate the percentage of finding a certain nanoparticle in a certain diameter. This confirmed that the size of nanoparticles decreases with increasing of the weight percentage of silver nanoparticles.

Evaluation of antibacterial activity

Antibacterial activities were evaluated using well diffusion method on Mueller-Hinton agar (MHA). The inhibition zones were reported in millimeter (mm). S. aureus and E. coli were used as references for the antibacterial assay. 18 to 24 hrs. single colonies on agar plates were used to prepare the bacterial suspension with the turbidity of 0.5 McFarland (equal to 1.5×108 colony-forming units (CFU)/ml). Briefly, MHA agar plates were inoculated with bacterial strain under aseptic conditions .The wells (diameter= 8mm) were filled with 80 µl of the test samples and incubated at 37 $^{\circ}$C for 24 hours. After the incubation period, the diameter of the growth inhibition zones was measured. All specimens (1, 2, 3, 4, 5 and 6) that depict PPy nanoparticles and PPy/Ag (0.1%, 0.5%, 3%, 5% and 7% wt.) nanocomposites exhibited an effectiveness against Gram-negative Escherichia coli showing an inhibition zone of 4mm and displayed poor efficacy against Gram-positive Staphylococcus aureus except for (5 and 6) which stand for PPy/Ag (5%, 7% wt.) that yield an inhibition zone of 4mm. This result agrees with M. Ghorbani et al. [25]. Fig.6 illustrates efficiency mechanism described above.

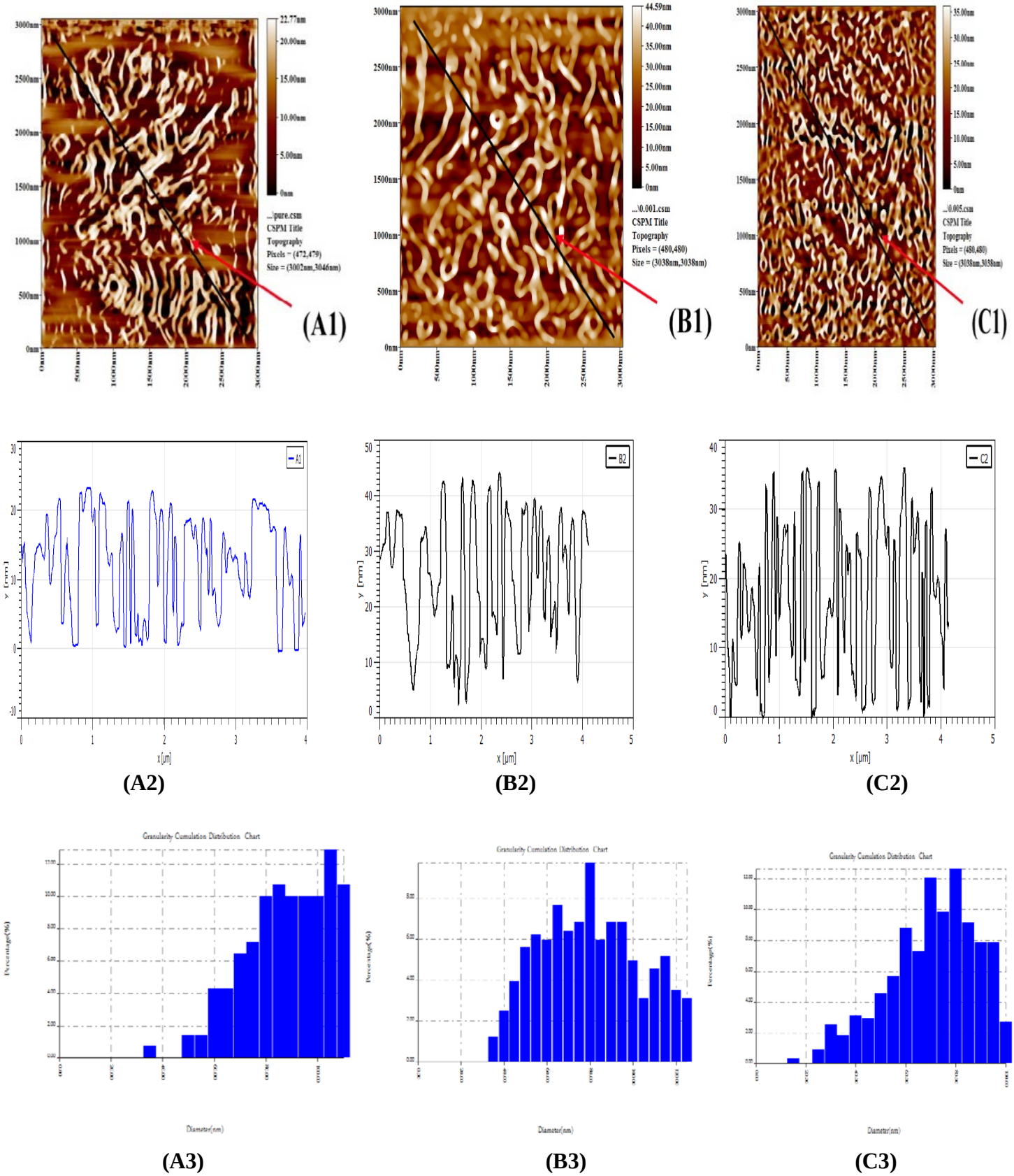

Fig. 5: (A1, B1, C1) AFM images of pure PPy particles, PPy/ 0.1%Ag and PPy/0.5%Ag nanocomposites. (A2, B2, C2) corresponding to width-height diagrams obtained by analysis of pictures A1, B1 and C1. (A3, B3, C3) size distribution chart.

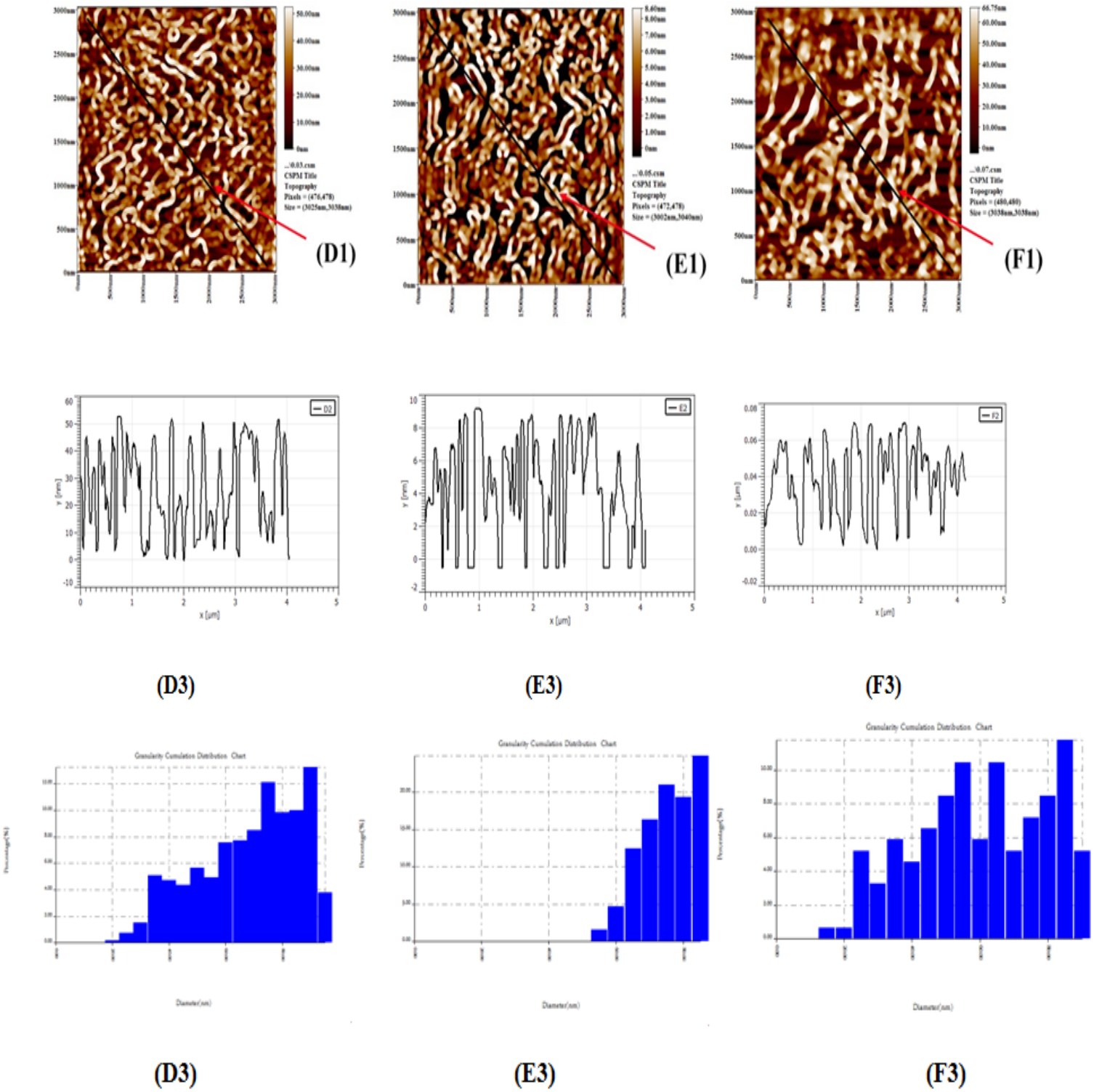

Fig. 5: (D1, E1, F1) AFM images of PPy/Ag (3%, 5% and 7% wt.). (D2, E2, F2) corresponding to width-height diagrams obtained by analysis of pictures D1, E1 and F1. (D3, E3, F3) size distribution chart.

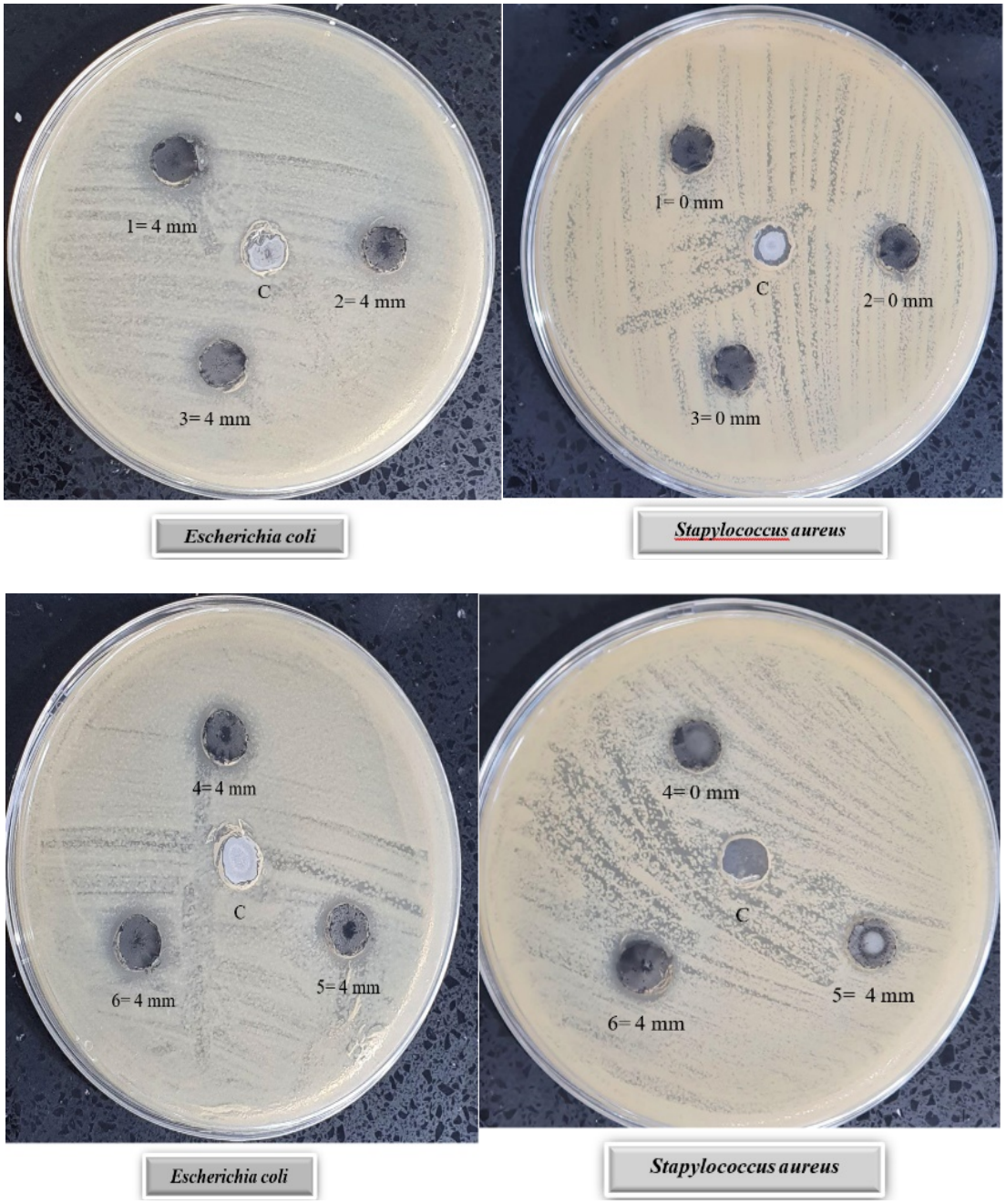

Fig. 6: Inhibition zones of PPy and PPy/Ag nanocomposites against (a) E. coli and (b) S. aureus.

Conclusions

The results of AFM measurements suggested the successful preparation of the PPy/ Ag nanocomposite. The results indicated that as the concentration of Ag in the nanocomposite increases, the roughness increases. The size of nanoparticles was also evaluated and found to be in the range of 15 nm to 125 nm. PPy/Ag nanocomposites exhibited an effectiveness against Gram-negative Escherichia coli showing an inhibition zone of 4mm but displayed poor efficacy against Gram-positive Staphylococcus aureus. The present mechanism could be adapted for the synthesis of other conductive polymer / metallic nanoparticles and these nanocomposites might be used as candidates in biological applications for their effective antimicrobial applications.

Acknowledgement

The authors wish to thank Assist. Prof. Amer Faisal Abdilamer, Department of Physics, University of Baghdad for his valuable assistance and helpful advice throughout this work.

References

[1] L. Ruiz-Pérez, L. Rizzello, J. Wang, N. Li, G. Battaglia, Y. Pei, Soft Matter, 16, 19 (2020) 4569-4573.
[2] K. Lota, G. Lota, A. Sierczynska, I. Acznik, Synth. Met., 203 (2015) 44-48.
[3] T. Hasani and H. Eisazadeh, Synth. Met., 175 (2013) 15-20.
[4] A. El Jaouhari, A. El Asbahani, M. Bouabdallaoui, Synth. Met., 226 (2017) 15-24.
[5] E. Karaca, K. Pekmez, N. Ö. Pekmez, Electrochim. Acta, 273 (2018) 379-391.
[6] A. R. Sadrolhosseini, M. Naseri, H. M. Kamari, Opt. Commun., 383 (2017) 132-137.
[7] A. M. Nowicka, M. Fau, T. Rapecki, M. Donten, Electrochim. Acta, 140 (2014) 65-71.
[8] E. M. Ryan and C. B. Breslin, Electrochim. Acta, 296 (2019) 848-855.
[9] H. Mansouri Torshizi, S. Zareian-Jahromi, M. Saeidifar, A. Ghasemi, H. Ghaemi, A. Heydari, Iran. J. Chem. Chem. Eng., 36, 5 (2017) 43-54.
[10] E. N. Zare, M. M. Lakouraj, M. Mohseni, Synth. Met., 187 (2014) 9-16.
[11] S. S. Pandey, S. Annapoorni, B. D. Malhotra, Macromolecules, 26, 12 (199) 3190-3193.
[12] H. Eisazadeh and M. Ghorbani, J. Vinyl Addit. Technol., 15, 3 (2009) 204-210.
[13] Z. T. Kolaei and H. Eisazadeh, Polym. Plast. Technol. Eng., 50, 14 (2011) 1438-1442.
[14] N. Asaadi, M. Parhizkar, S. Mohammadi Aref, H. Bidadi, Iran. J. Chem. Chem. Eng., 36, 3 (2017) 65-72.
[15] N. Yousefi, M. Pazouki, F. Alikhani Hesari, M. Alizadeh, Iran. J. Chem. Chem. Eng., 35, 2 (2016) 51-62.
[16] S. Gurunathan, J. H. Park, J. W. Han, J.-H. Kim, Int. J. Nanomedicine, 10 (2015) 4203-4223.
[17] W.-R. Li, X.-B. Xie, Q.-S. Shi, H.-Y. Zeng, O.-Y. You-Sheng, Y.-B. Chen, Appl. Microbiol. Biotechnol., 85, 4 (2010) 1115-1122.
[18] S. Horike, D. Umeyama, S. Kitagawa, Acc. Chem. Res., 46, 11 (2013) 2376-2384.
[19] A. Salabat, F. Mirhoseini, M. Arjomandzadegan, E. Jiryaei, New J. Chem., 41, 21 (2017) 12892-12900.
[20] W. R. Salanak, R. Erlandssom, J. Priza, I. Lundatrom, O. Inganas, Synth. Met., 5 (1983) 125-139.
[21] S. T. Navale, A. T. Mane, M. A. Chougule, R. D. Sakhare, S. R. Nalage, V. B. Patil, Synth. Met., 189 (2014) 94-99.
[22] M. D. Bedre, S. Basavaraja, R. Deshpande, D. S. Balaji, A. Venkataraman, Int. J. Polym. Mater, 59, 8 (2010) 531-543.
[23] M. T. Ramesan, J. Appl. Polym. Sci., 128, 3 (2013) 1540-1546.
[24] J. Joseph and D. C. Trivedi, Bull. Electrochem., 4 (1988) 469-471.
[25] M. Ghorbani, A. Ehsani, M. Soleimani, Iran. J. Chem. Chem. Eng., 38, 3 (2019) 1-7.